Journal of the Mechanical Behavior of Biomedical Materials 74 (2017) 383–391

Contents lists available at ScienceDirect

Journal of the Mechanical Behavior of Biomedical Materials

journal homepage: www.elsevier.com/locate/jmbbm

In vitro degradation of a 3D porous *Pennisetum purpureum*/PLA biocomposite scaffold

R. Revati[a], M.S. Abdul Majid[a,*], M.J.M. Ridzuan[a], K.S. Basaruddin[a], M.N. Rahman Y.[a], E.M. Cheng[a], A.G. Gibson[b]

[a] School of Mechatronic Engineering, Universiti Malaysia Perlis (UniMAP), Pauh Putra Campus, 02600 Arau, Perlis, Malaysia
[b] School of Mechanical and Systems Engineering, Newcastle University, Newcastle upon Tyne NE1 7RU, UK

ARTICLE INFO

Keywords:
Tissue engineering
Scaffold
Polylactic acid
Biodegradation
Mechanical properties

ABSTRACT

The *in vitro* degradation and mechanical properties of a 3D porous *Pennisetum purpureum* (PP)/polylactic acid (PLA)-based scaffold were investigated. In this study, composite scaffolds with PP to PLA ratios of 0%, 10%, 20%, and 30% were immersed in a PBS solution at 37 °C for 40 days. Compression tests were conducted to evaluate the compressive strength and modulus of the scaffolds, according to ASTM F451-95. The compression strength of the scaffolds was found to increase from 1.94 to 9.32 MPa, while the compressive modulus increased from 1.73 to 5.25 MPa as the fillers' content increased from 0 wt% to 30 wt%. Moreover, field emission scanning electron microscopy (FESEM) and X-ray diffraction were employed to observe and analyse the microstructure and fibre-matrix interface. Interestingly, the degradation rate was reduced for the PLA/PP_{20} scaffold, though insignificantly, this could be attributed to the improved mechanical properties and stronger fibre-matrix interface. Microstructure changes after degradation were observed using FESEM. The FESEM results indicated that a strong fibre-matrix interface was formed in the PLA/PP_{20} scaffold, which reflected the addition of *P. purpureum* into PLA decreasing the degradation rate compared to in pure PLA scaffolds. The results suggest that the *P. purpureum*/PLA scaffold degradation rate can be altered and controlled to meet requirements imposed by a given tissue engineering application.

1. Introduction

Various biodegradable polymers have been utilised to produce scaffolds in tissue engineering. These microstructures maintain the extracellular matrix (ECM)[1] production by cells and are presumed to evenly degrade, allowing the surrounding tissue to recover the supporting function of the scaffold (Chen et al., 2002). Biodegradable polymers are used to provide temporary support for cell growth and the chemical properties of these polymers allow hydrolytic degradation through de-esterification (Cordonnier et al., 2011). Once degraded, the monomeric components of each polymer are removed by natural pathways (Tian et al., 2012). The biological performance of biomaterials highly depends on their degradation behaviour, owing to the influence of degradation on cell performance and inflammatory response (Fakhrul and Islam, 2013; Hetal Patel, 2011; Razak et al., 2012). Therefore, it is crucial to investigate the degradation behaviour of biodegradable materials, as the degradation rate is an important factor affecting cartilage tissue regeneration.

In order to produce enhanced engineering of cartilage tissue constructs, an ideal cartilage tissue engineering scaffold should have both sufficient biochemical and physical properties similar to natural cartilage with favourable chemical composition and biological properties that primarily influence nutrient transfer, waste removal, cell attachment, differentiation, and proliferation (Tu et al., 2003; Vogt et al., 2002; Zhang et al., 2009). Although the material modification can improve the mechanical modulus values of scaffolds, material properties should allow for continuous hydrolytic attack and degradation of the temporary scaffold (Zhang and Cui, 2012). Various techniques have been used to enhance surface cell attachment and bioactivity of synthetic polymers, such as blending with hydrophilic materials including chitosan (Zhu et al., 2013), collagen (Chen et al., 2012), alginate (Jeong et al., 2010), and hydroxyapatite (Shah et al., 2011).

Composites composed of a biodegradable polymeric matrix with organic fillers exhibit considerable promise in the field of orthopaedic

* Corresponding author.
E-mail addresses: revark_1990@yahoo.com (R. Revati), shukry@unimap.edu.my (M.S.A. Majid), ridzuanjamir@unimap.edu.my (M.J.M. Ridzuan), khsalleh@unimap.edu.my (K.S. Basaruddin), nurrahman@unimap.edu.my (M.N. Rahman Y.), emcheng@unimap.edu.my (E.M. Cheng), geoff.gibson@ncl.ac.uk (A.G. Gibson).

[1] Abbreviations: ECM-extracellular matrix; EVOH- ethylene vinyl alcohol copolymer; FESEM-field emission scanning electron microscopy; NaCl-sodium chloride; PLA- polylactic acid; PP- Pennisetum purpureum.

http://dx.doi.org/10.1016/j.jmbbm.2017.06.035
Received 21 March 2017; Received in revised form 23 June 2017; Accepted 26 June 2017
Available online 27 June 2017

regenerative medicine since they can provide improved mechanical properties and enhanced interaction with host tissue (Olivas-armendariz et al., 2015). Polylactic acid (PLA), an aliphatic polyester, has been evaluated as a potential biomaterial for cartilage regeneration owing to its good biocompatibility and biodegradability (Gupta et al., 2007; Hoveizi et al., 2014; Lopes et al., 2012). However, PLA has poor mechanical strength and its surface does not promote cell adhesion. Due to its ability to enhance osteoinductivity and osteoconductivity, natural fibres are frequently used with PLA as a scaffold material for tissue engineering (AL-Oqla et al., 2015; Bogoeva-Gaceva et al., 2007). Incorporation of natural fibres with PLA can overcome the deficiency of hydrophobicity of PLA and improve the mechanical properties of the scaffolds (Chandramohan, 2011).

Pennisetum purpureum fiber, also commonly known as Napier grass, is mainly composed of 46% cellulose, 34% hemicellulose, and 20% lignin (Haameem et al., 2016). This fibre is a plant that forms robust bamboo-like clumps and is locally sustainable throughout Malaysia. The use of *P. purpureum* reinforced composites consist of many benefits includes excellent biodegradability, adequate specific strengths and moduli, and economized tool wear (Ridzuan et al., 2016). Utilisation of *P. purpureum* as a reinforcement filler in a PLA matrix offers many advantages; it results in the production of biocomposites with favourable mechanical properties and controllable biodegradability. Ridzuan et al. determined that *P. purpureum* fibres could potentially be used as reinforcement materials in polymer composites. They determined that the application of alkaline treatment on fibres can effectively increase the surface roughness and minimises the hemicelluloses quantities of the fibre (Ridzuan et al., 2016). Hameem et al. studied the tensile and flexural properties of *P. purpureum* and concluded that when polyester composites were reinforced with *P. purpureum*, their mechanical properties improved (Haameem et al., 2016). Similarly, Ridzuan et al. reported that moisture absorption influences the mechanical properties of hybrid *P. purpureum*/glass–epoxy composites (Ridzuan et al., 2016). They noticed that as the glass fibre content of the samples increased, the degree of moisture absorption decreased while the tensile and flexural strength of the composites increased. Based on several recent studies, it can be suggested that *P. purpureum* fibres could be used effectively as reinforcement filler in polymer composites for cartilage tissue engineering applications (Haameem et al., 2016; Ridzuan et al., 2016; Ridzuan et al., 2016; Ridzuan et al., 2016; Haameem et al., 2016).

In this study, we evaluated *in vitro* degradation behaviours of the PLA and *P. purpureum*/PLA scaffolds. For the study of their *in vitro* degradation behaviour, the composite scaffolds were immersed in PBS. To observe the effect of the PBS solution pH on the degradation behaviour of the scaffolds, the scaffold-immersed buffer solution was not changed until the experiment was ended (pH was evenly lowered by the formation of acid due to the degradation of PLA). In addition, the surface morphology and mechanical properties of *P. purpureum*/PLA scaffolds, influenced by various filler compositions, were investigated in order to mimic conditions in the human body.

2. Materials and methods

2.1. Materials

The biocomposite scaffolds were fabricated using *P. purpureum* fibre, PLA, chloroform, and dichloromethane. *P. purpureum* grass was purchased from a local plantation located at Bukit Kayu Hitam, Kedah, in northern peninsular Malaysia. PLA pellets were purchased from NatureWork LLC. Chloroform and dichloromethane were used as organic solvents and were mixed in a ratio of 1:1. Analytical grade sodium chloride (NaCl) was used as the porogen in this study.

2.2. Extraction and preparation of P. purpureum powder

P. purpureum fibres were extracted from the grass stems internodes using water retting process. The *P. purpureum* grass was cleaned and crushed before being immersed in a tank filled with tap water for 2–3 weeks. The fibres were extracted manually from stems and cleaned using distilled water. The extracted fibres were then sun-dried to eliminate excess moisture content within the fibres. The extracted dried *P. purpureum* fibres were treated using NaOH solution with a concentration of 5 wt% (Haameem et al., 2016). Subsequently, the *P. purpureum* fibres were cut into smaller forms before proceeding with grinding and sieving in order to convert the *P. purpureum* fibre into powder form. The process of grinding and sieving was repeated several times to produce a fine powder. The size of the powder obtained from the sieving process ranged from 9 to 36 μm when observed under FESEM.

2.3. Fabrication of P. purpureum/PLA composite scaffolds

P. purpureum/PLA composite scaffolds were prepared by the solvent casting and particulate leaching method. First, the PLA pellets were dissolved in chloroform and dichloromethane (volume ratio 1:1) to a final concentration of 60.0 mg/mL. Then, different concentrations of *P. purpureum* (10%, 20%, and 30% of PLA weight basis) were added to the above PLA solution, and the mixture was agitated via a magnetic stirrer for 2 h at a constant temperature of 70 °C. NaCl was further added to the solution and stirred for another 20–30 min to obtain a homogenous solution. The PLA composite solution and NaCl was mixed in a ratio of 1:9. Next, the NaCl-PLA composite solution was poured into a Teflon mold and further dried at room temperature overnight. Finally, the composites were leached with distilled water for 48 h to eliminate the salt particles in the composites and the *P. purpureum*/PLA composite scaffolds were obtained. The control, pure PLA scaffold, was prepared using the same fabrication technique.

2.4. Field-emission scanning electron microscopy (FESEM) analysis

The composite scaffolds were vacuum-dried and their surface was prepared for observation with FESEM at the initial and final stage of the observation period. The prepared specimens were cut using a scalpel to reveal the cross section of the scaffolds. The cross section of the PP/PLA scaffolds were then platinum coated using a sputter coater (Quorum, Q150R S). The morphology of the composite scaffolds was observed with FESEM-NOVA NanoSEM 450, operated at the voltage of 3 kV.

2.5. X-ray diffraction analysis (XRD)

To conduct the XRD analysis, the prepared specimens were further cut with dimension of 20 mm diameter and 1 mm thickness. The phase composition of the samples was analysed by XRD (Shimadzu Lab X XRD-6000 diffractometer). This equipment operates with current and voltage settings of 30 mA and 40 kV, respectively, and uses Cu radiation (1.54060 Å). The XRD diagrams of the samples were recorded in the interval $10^\circ \leq 2\theta \leq 80^\circ$ at a scan speed of 4°/min with the step size 0.02 and the step time 0.24 s.

2.6. Mechanical characterisation

In accordance with ASTM F451-95, compression tests were performed on both PLA and *P. purpureum*/PLA composite scaffolds to evaluate the effects of adding *P. purpureum* fibres to scaffolds. Resistance to mechanical compression of the composite scaffolds was tested on an Instron Microtester 5848 equipped with a 10.0 kN load cell at room temperature. Rectangular-shaped samples measuring 13 mm in length, 25 mm in thickness, and 13 mm in width were used. The crosshead speed was set at 1.0 mm min^{-1}, and the load was applied until the sample was compressed to 80% of its initial height. The maximum point of the stress-strain curve was estimated as the compressive strength of the scaffold. The compressive modulus of the

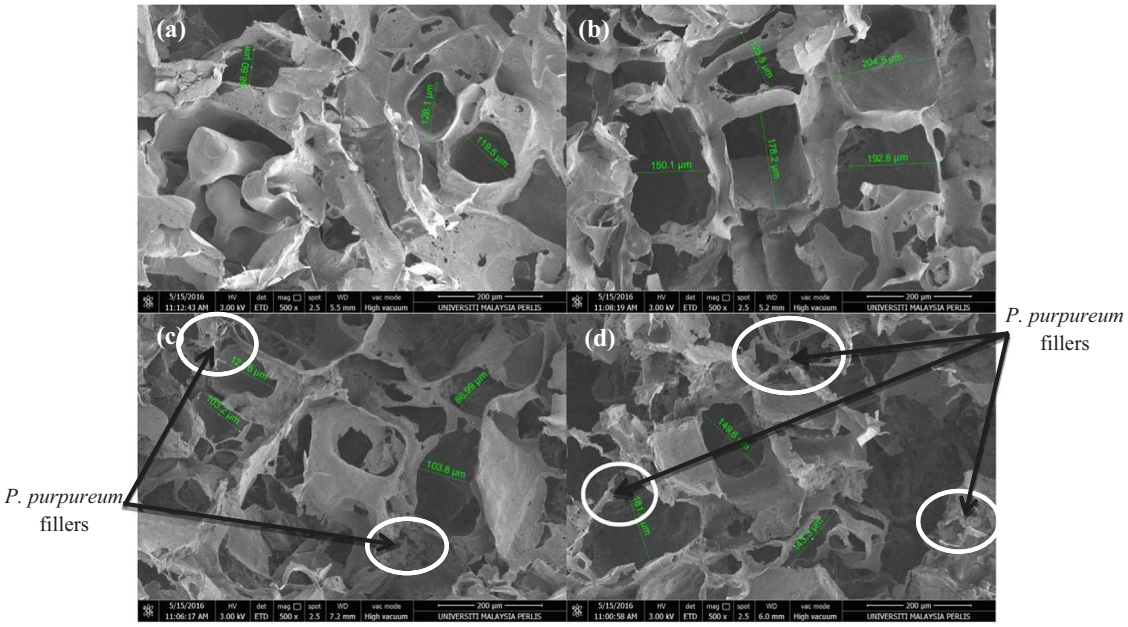

Fig. 1. FESEM images of porous *P. purpureum*/PLA scaffolds with microscale pores: (a) PLA_C, (b) PLA/PP_{10}, (c) PLA/PP_{20}, and (d) PLA/PP_{30}.

composite scaffolds was computed from the slope of the initial linear portion of the stress-strain curve. Three samples were tested for each composition and the average values were reported. The morphology of the compressed samples was analysed by FESEM-NOVA NanoSEM 450 to evaluate the effect of compression on the microstructure of the scaffolds.

2.7. In vitro degradation of P. purpureum/PLA composite scaffolds

2.7.1. Sample preparation

Prior to degradation, the *P. purpureum*/PLA were pre-wetted to make sure that the PBS solution penetrated through all the pores of the composite scaffolds (Wu and Ding, 2004). The prepared scaffolds were pre-wetted by immersing the samples in ethanol for 1 h and then transferred into buffer (PBS) solution for 1 h; due to the hydrophobic character of PLA, the composite scaffolds cannot be directly immersed in the PBS solution (Oh et al., 2006). Various *P. purpureum*/PLA composite scaffolds and a pure PLA scaffold were prepared as a rectangle with a length of 13 mm, width of 13 mm, and thickness of 25 mm. The samples were immersed in glass vials containing 20 ml of PBS solution and were placed in a 37 °C incubator. The *in vitro* degradation of the scaffolds was further evaluated by pH changes, weight loss, and water uptake testing using a PBS solution (0.1 M, pH 7.4) as degradation medium. All experiments were carried out in an incubator (37 °C) and the degradation period lasted for 40 days.

2.7.2. pH changes of degradation medium

The measurement of pH changes was performed by immersing the composite scaffolds in a PBS solution (pH 7.4) for up to 40 days. The degradation medium was not refreshed throughout the degradation period. The pH of the degradation medium was measured every 5 days using a pH meter (Model H1 2213 pH/ORD HANNA Instrument). Three samples were prepared for each composition and the average pH of three samples was reported.

2.7.3. Water uptake and weight loss of P. purpureum/PLA scaffolds

The measurement of water uptake and weight loss was carried out by immersing the composite scaffolds in a PBS solution at 37 °C for up to 40 days. At the end of each time point, the weight of the swollen samples was measured after removing the excess surface water with filter paper. The water uptake percentage of the scaffolds was determined from weight of wet sample (w_w) and the initial weight of dry sample (w_i) using the following Eq. (1). The reported water uptake was considered as the average value of three samples.

$$Wateruptake(\%) = \frac{(W_w - W_i)}{W_i} \times 100 \quad (1)$$

The weight loss of the scaffolds was determined from the initial weight of dry sample (w_i) and weight of final dry sample (w_f) at the end of each time point using Eq. (2)

$$Weightloss(\%) = \frac{(W_i - W_f)}{W_i} \times 100 \quad (2)$$

At the end of predetermined time intervals, all samples from each composition were removed and weighed to calculate the percentage of water uptake (Eq. (1)), washed thoroughly with distilled water to eliminate any soluble inorganic salt, and weighed after being completely vacuum dried at room temperature to a constant weight for calculation of the percentage of weight loss (Eq. (2)).

2.7.4. Analysis of sample morphology by FESEM

The morphology of the samples after 40 days of degradation was examined using FESEM-NOVA NanoSEM 450. For FESEM observation, the degraded samples were coated with platinum using a sputter coater.

3. Results and discussion

3.1. FESEM analysis

The appropriate microstructure of pores is the crucial point to maximise the efficiency of a scaffold, in combination with pore size, porosity, and interconnected pores. In fact, it has been emphasised that the scaffold needs to be highly porous with the ideal pore size in order to enhance migration and proliferation of cells in tissue engineering. Pore microstructure also strongly influences the vascularisation and permeability of the scaffold for the transportation of oxygen/nutrients and the removal of waste products (Naseri et al., 2016).

FESEM observation of the synthesised PLA and prepared composite scaffold (PLA_C, PLA/PP_{10}, PLA/PP_{20}, and PLA/PP_{30}) is shown in Fig. 1. The figure shows that the scaffold contains uniformly distributed pores that are well-interconnected and approximately of a constant pore size with a thinner wall structure. The pore size of the pure PLA scaffold was

around 68 to 128 μm (Fig. 1a). In *P. purpureum*/PLA scaffolds, the pore size varied from 87 to 204 μm as measured by FESEM (Fig. 1b-d). These results illustrated that as the content of *P. purpureum* increased, a rougher, irregular pore shape, and thinner wall structure with significant pores was observed compared to PLA_C and PLA/PP_{10}, which was considered encouraging for the pore size required for cartilage applications. Proper pore size is the key point in determining the efficiency of a scaffold; very small pores prohibit penetration of cells into scaffolds, and very large pores prohibit recruitment of cells due to lack of colonisation in the area by cells (Gentile et al., 2014).

FESEM images of *P. Purpureum*/PLA scaffolds showed that the fillers were uniformly distributed in the composite scaffolds. These results suggest that up to 10% *P. purpureum* content does not influence the mechanism of pore formation via the solvent casting and particulate leaching technique. However, once the *P. purpureum* content increases to 20% and 30%, the microstructure of the composite scaffolds appears to differ from the other two scaffolds. Scaffolds with macro- and micro-sized structures identical to that of natural cartilage are important. An ideal scaffold should mimic the structure and function of a natural ECM as far as possible (Cen et al., 2008).

Table 1 shows the porosity of the scaffolds. With the addition of *P. purpureum,* the porosity of the scaffolds decreased from 99.6% to 99.1% (Revati et al., 2017). The compact arrangement of the filler in polymer scaffolds was a possible cause for the denser microstructure of *P. purpureum*/PLA scaffolds. In this study, 10% of *P. purpureum* content did not distinctly change the porosity of the scaffold. However, increasing the filler content by up to 30% slightly decreased the porosity of the composite scaffolds. Based on a literature review, the porosity should be influenced by the amount of reinforced fillers added into the polymer matrix (Cheung et al., 2009).

Similarly, Huang et al., (2010) illustrated that the addition of microspheres up to 50% did not noticeably change the porosity of the PHBV-PLGA scaffolds. An ideal scaffold with satisfactory porosity can be achieved by obtaining porosity of more than 80%. The porosity of PLA with and without *P. purpureum* was all beyond 99%. It can be concluded that the addition of fillers improved structural stability of the scaffold, which is crucial to endure stress generated during *in vitro* and *in vivo* cell culturing.

3.2. X-ray diffraction analysis

The effect of *P. purpureum* fibres on the microstructure and morphology of a porous PLA scaffold and its composite scaffolds was analysed by XRD. Fig. 2 shows the X-ray diffractograms of the PLA and composite scaffolds. In all compositions, a major semi-crystalline peak at $2\theta \approx 17.6^{\circ}$ was observed without the presence of any crystalline peaks related to *P. purpureum* fibres. Interestingly, we did not observe any *P. purpureum* related peaks, even in high fibre content. Similarly, Ramesh et al. studied the X-ray diffraction of the electrospun ethylene vinyl alcohol copolymer (EVOH) reinforced with PLA. They did not observe any EVOH related peaks, even in the case of high EVOH content (Neppalli et al., 2013).

The XRD patterns for the PLA_C scaffold exhibited a broad diffraction peak centred at $2\theta \approx 17.66^{\circ}$. The PLA_C did not show any other characteristic peak, which indicates that the microstructure of the scaffold is semi-crystalline, similar to that described by Hong and co-workers

Table 1
Composition, porosity, and average pore size of the *P. purpureum*/PLA scaffolds.

Copolymer Samples	PLA_C	PLA/PP_{10}	PLA/PP_{20}	PLA/PP_{30}
PLA (g)	2.4	2.4	2.4	2.4
P. purpureum (g)	0.00	0.24	0.48	0.72
Average pore size (μm)	105 ± 36	170 ± 45	103 ± 21	158 ± 23
Porosity (%)	99.6 ± 0.26	99.4 ± 0.20	99.1 ± 0.29	99.2 ± 0.37

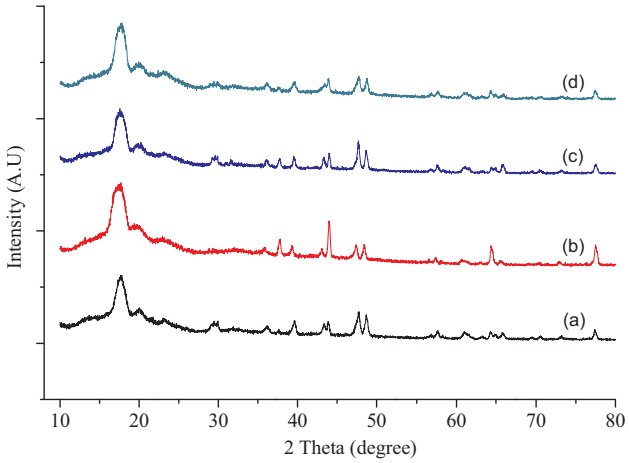

Fig. 2. X-ray diffraction patterns of porous *P. purpureum*/PLA scaffolds: (a) PLA_C, (b) PLA/PP_{10}, (c) PLA/PP_{20}, and (d) PLA/PP_{30}.

(Hong et al., 2008). The PLA_C scaffold employed in this research had 4.93 Å of interlayer spacing at $2\theta \approx 17.66^{\circ}$. The XRD pattern of the PLA/PP_{10}, PLA/PP_{20}, and PLA/PP_{30} scaffolds had a very similar semi-crystalline peak at 2θ of 17.68°, 17.56°, and 17.68°, which corresponded to the basal spacing of 4.96 Å, 5.01 Å, and 5.06 Å, respectively. The shift to a higher angle signified an increase in the corresponding interlayer spacing, which is supported by the fact that the composite scaffolds had an ordered structure. Based on the information presented in Fig. 2, as the PLA chain was the majority of the blend, the position of the crystalline peak was almost identical to that of the *P. purpureum*/PLA scaffolds with varying filler content.

Two factors seem to influence the degree of crystallinity: the presence of the *P. purpureum* fibres and the content of fibre that determine the strength of the fibre-matrix interface. The controllability of the crystalline structure is expected to impact the mechanical performance and degradation rate of the scaffold, providing a broader range of properties that can be controlled to influence the scaffold performance by varying the composition of *P. purpureum* content. Overall, *P. purpureum*/PLA scaffolds exhibit similar diffraction patterns, supporting the idea they possess similar microstructure and similar compositions.

3.3. Mechanical characterisation

The load-bearing nature of the cartilage in which the engineered scaffold will be implanted is considered important when designing the mechanical properties of the scaffold. Design considerations for mechanical strength will rely upon whether the scaffold will be utilised as a part of an *in vitro* or *in vivo* application. If the scaffold will be embedded into an articular joint *in vivo* right after fabrication, its mechanical characterisation should be a perfect match for those of native cartilage to support the loads experienced in the joint. The optimum force applied to the knee cartilage during ordinary physiological loading ranges from 1.9 to 7.2 times body weight (Komistek et al., 2005), which relates to around 0.84 to 3 MPa for a 70 kg individual (Izadifar et al., 2012).

The compression strength and modulus of PLA_C, PLA/PP_{10}, PLA/PP_{20}, and PLA/PP_{30} are given in Figs. 3(a) and (b). The compressive strength of the PLA/PP_{30} (9.32 ± 0.46 MPa) scaffold was noticeably higher than that of the PLA_C (1.94 ± 0.09 MPa), PLA/PP_{10} (4.33 ± 0.21 MPa), and PLA/PP_{20} (7.49 ± 0.37 MPa) scaffolds. Additionally, the compressive modulus of the PLA/PP_{30} (5.25 ± 0.26 MPa) scaffold was significantly higher than that of the PLA_C (1.73 ± 0.08 MPa), PLA/PP_{10} (2.75 ± 0.13 MPa), and PLA/PP_{20} (3.72 ± 0.18 MPa) scaffolds. The compression strength of the *P. purpureum*/PLA scaffolds increased as the composition of filler increased. Moreover, the compressive modulus of the *P. purpureum*/PLA scaffolds

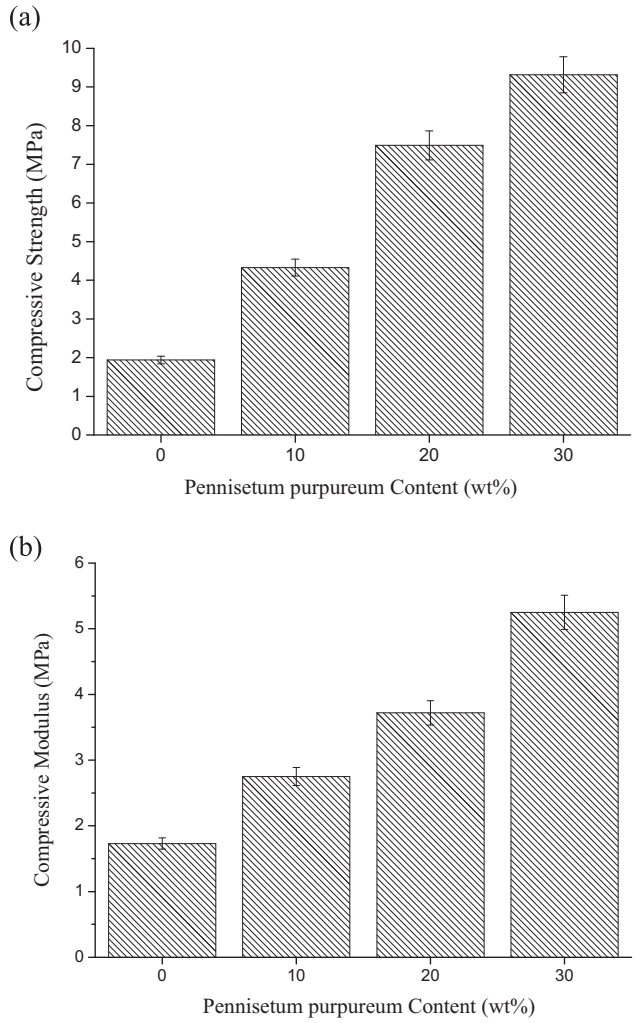

Fig. 3. (a) Compressive strength and (b) compressive modulus of porous *P. purpureum*/PLA scaffolds with different *P. purpureum* contents.

proves that the addition of *P. purpureum* can improve the mechanical properties of the scaffolds without influencing the porosity. It is well known that it is challenging to achieve high compressive strength and modulus for porous scaffolds because of the negative impacts gained from a porous structure. However, in this case, the increased compressive strength and modulus of the scaffold was achieved by increasing the *P. purpureum* composition while maintaining the targeted scaffold porosity (99%).

The images of pure PLA and *P. purpureum*/PLA scaffolds after compression testing were studied using FESEM, as shown in Fig. 4. Matrix fracture, fibre brittleness, and scaffold yielding could be observed after compression testing for composite scaffolds. The images in Fig. 4 clearly illustrate the fibre content on the compressed surface of the scaffolds. The PLA_C scaffold showed no significant changes in microstructure, irrespective of the number of compact layers or compression sequences. Lower *P. purpureum* content will lead to poor mechanical properties, owing to the fact that the load transferred from the matrix was supported by less fibre. The FESEM image in Fig. 4(c) shows the surface of the compressed scaffold for 20 wt% *P. purpureum* content. This image shows an improved, stronger bond between the matrix and the fibres compared to the other scaffolds, which results in a more effective load transfer along the fibre-matrix interface. As a result, an increase in the scaffold strength can be observed. A similar effect was also observed for the PLA/PP_{30} scaffold. However, the compact surface of the PLA/PP_{30} scaffold after compression testing showed *P. purpureum* fibre breakage in a more brittle manner, compared to that of the PLA/PP_{20} scaffold, as can be observed in Fig. 4(c) and (d). In general, compression of *P. purpureum*/PLA scaffolds results in a reduction of pore size; the corresponding PLA_C scaffold was minimally affected by compression (Fig. 4).

In this study, the PLA/PP_{20} and PLA/PP_{30} scaffolds have shown desirable compressive mechanical properties (3.7 and 5.2 MPa) to boost chondrogenesis, as well as encouraging pore sizes and morphology of pore microstructure for cell adhesion. These scaffolds are predicted to enhance the ECM and regenerate cartilage with the appropriate mechanical properties after implantation. However, further study of the scaffolds after the development of ECM will be necessary to predict the behaviour of the scaffolds *in vivo*, where the scaffolds will be further analysed for its biocompatibility and cytotoxicity.

3.4. In vitro degradation of *P. purpureum*/PLA composite scaffolds

3.4.1. Effect of *P. purpureum* on the pH changes in degradation medium

The change in pH value over the degradation period is presented in Fig. 5. Acidic groups resulting from the degradation of PLA may decrease the pH value of the degradation medium, while the dissolution of the *P. purpureum* fillers could alkalize the medium. Therefore, the pH of the PBS medium is highly dependent on both the degradation rate of the PLA matrix and the dissolution of the *P. purpureum* fillers. As shown in Fig. 5, the pH value of the degradation medium incubating the pure PLA scaffold decreased sharply through the 0–10th day and gradually increased throughout the rest of the degradation period and reached around 7.43 at the end of the 35th to 40th day of incubation. In addition, the pH value of the medium incubating the PLA/PP_{10} scaffold decreased at a fast rate through the 0–10th day and reached around 7.32 at the end of the 10th day of incubation. After the 10th day, the pH began to increase up to 7.40 at the end of the 40th day. Then, owed to the high molecular weight (M_W = 200,000) of PLA used in this study, it degraded quite fast, the pH of the degradation medium incubating the PLA/PP_{20} and PLA/PP_{30} scaffolds decreased sharply through the 0–15th day of incubation. Both scaffolds reached around 7.28 at the end of the 15th day of incubation, but after the 15th day, the pH began to waver. They exhibited an upward trend from the 20th day and reached 7.33 and 7.34 at the end of the 40th day of incubation, respectively.

The pH drops during the degradation time up to 10–15 days, releasing more acidic degradation products into the medium. After the initial 15 days of incubation, the pH value increases due to significant reduction of specimen size. PLA/PP_{20} and PLA/PP_{30} degradation resulted in a similar trend in pH changes as observed for PLA/PP_C and PLA/PP_{10}, except PLA/PP_{20} and PLA/PP_{30} scaffolds are slightly more acidic during the last 25 days compared to PLA/PP_C and PLA/PP_{10}. It could be concluded that based on the pH values obtained from the experiment, the PBS medium of PLA/PP_{20} and PLA/PP_{30} is more acidic compared to PLA/PP_C and PLA/PP_{10} due to the introduction of *P. purpureum* fillers in PBS medium.

3.4.2. Water uptake and weight loss of *P. purpureum*/PLA scaffolds

The scaffolds based on *P. purpureum* and PLA were prepared by the solvent casting and particulate leaching methods. The key point in the *in vitro* degradation studies was the osmolarity and ion concentration of PBS solution which matches with the human body for stimulating physiological conditions, which are responsible for the degradation of the *P. purpureum*/PLA scaffolds. Degradation with PBS medium was performed under incubation. The water permeability of a scaffold and its ability to absorb water influence the absorption of cell culture medium or physiologically relevant buffers and the transportation of cell nutrients and metabolites throughout the scaffold. The PBS uptake of the scaffold material and that of the structure give various measures of the ability of the scaffold to bind to fluid.

Fig. 6 shows the water uptake of the *P. purpureum*/PLA scaffolds with different *P. purpureum* content. According to the results, the

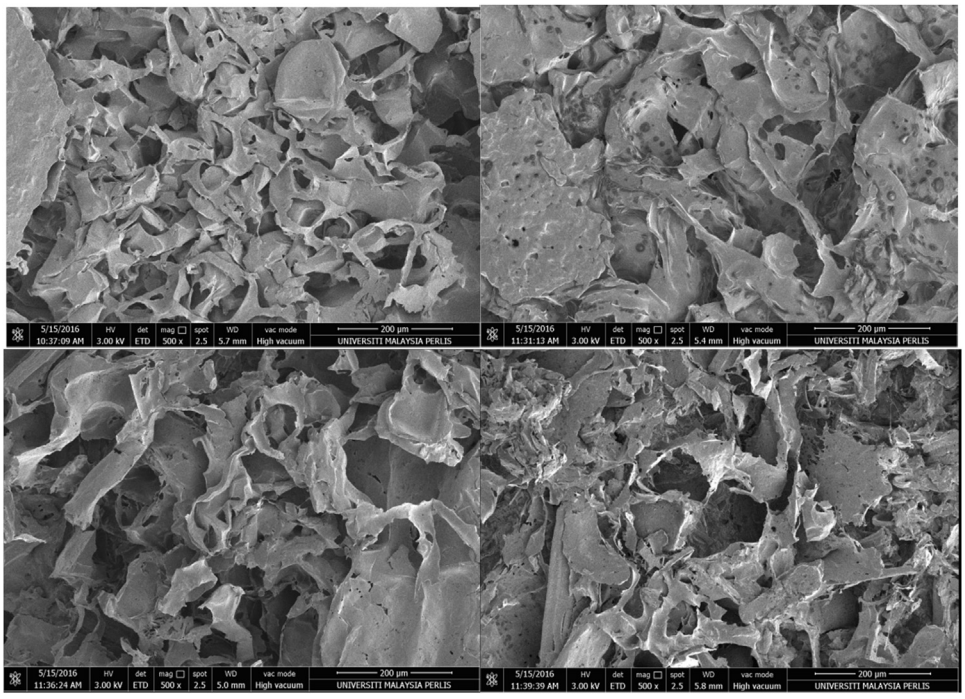

Fig. 4. FESEM images of porous *P. purpureum*/PLA scaffolds after compression: (a) PLA_C, (b) PLA/PP_{10}, (c) PLA/PP_{20} and (d) PLA/PP_{30}.

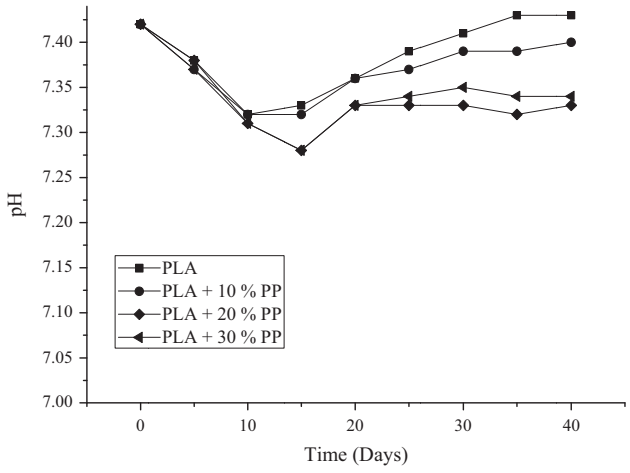

Fig. 5. pH changes vs. incubation time in PBS for porous *P. purpureum*/PLA scaffolds: (a) PLA_C, (b) PLA/PP_{10}, (c) PLA/PP_{20}, and (d) PLA/PP_{30}.

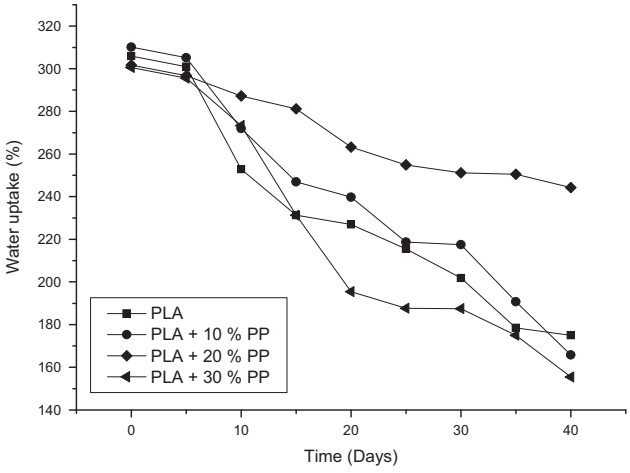

Fig. 6. Water uptake vs. incubation time in PBS for porous *P. purpureum*/PLA scaffolds: (a) PLA_C, (b) PLA/PP_{10}, (c) PLA/PP_{20}, and (d) PLA/PP_{30}.

percentage of water uptake is decreased throughout the degradation period. Compared to the PLA/PP_{20} scaffold, the water content of the PLA_C, PLA/PP_{10}, and PLA/PP_{30} scaffolds decreased rapidly after the immersion of scaffolds in medium, even with the hydrophilic behaviour of the added *P. purpureum* fillers. However, the water uptake of the biocomposite scaffolds decreased remarkably in the presence of PBS medium (Fig. 6), which was due to the higher degree of crystallinity and also to the lower dispersity of PLA.

The PLA/PP_{20} scaffold shows that the percentage of water uptake decreased slowly and reached around 245%, compared to that of the PLA_C, PLA/PP_{10}, and PLA/PP_{30} scaffolds, which decreased significantly and reached around 175%, 165%, and 155%, respectively. The PLA/PP_{20} composite scaffold exhibited the highest water absorption percentage throughout the whole incubation period. The water uptake ability of the *P. purpureum*/PLA scaffold gradually increased with further addition of *P. purpureum* content due to the presence of *P. purpureum* fillers on the surface of the composite scaffold. As a cellulose fibre, *P. purpureum* is naturally hydrophilic and its presence within the scaffold can significantly enhance the water absorption ability of scaffold. In contrast, the PLA/PP_{30} scaffold showed that the percentage of water uptake decreased rapidly, compared to the PLA/PP_{20} scaffold, owing to the weakness of the fillers to protrude from the surface of the scaffolds. This result agrees with the result of the weight loss analysis (Fig. 7).

In tissue engineering, it is expected that the degradation rate of *P. purpureum*/PLA scaffolds controls the regeneration and repair process of tissue. This is achieved by modifying the composition of the polymer composites. However, it is compulsory to highlight the influence of *P. purpureum* on the *in vitro* degradation behaviour of scaffolds, as the degradation rate is a critical factor affecting the recovery of damaged cartilage. The degradation mechanism of biodegradable polymers is chemical degradation; it was observed that the chain ends cleavage resulted in weight loss, while the random scission influenced the reduction in weight loss. Therefore, water absorption is considered to be particularly important for the degradation of the scaffold (as illustrated in Fig. 6). The weight loss for the different porous *P. purpureum*/PLA scaffolds after incubation in PBS is shown in Fig. 7. The weight loss of the PLA/PP_{20} scaffold proceeded slowly throughout the whole degradation period. After 40 days of incubation, the scaffold lost about

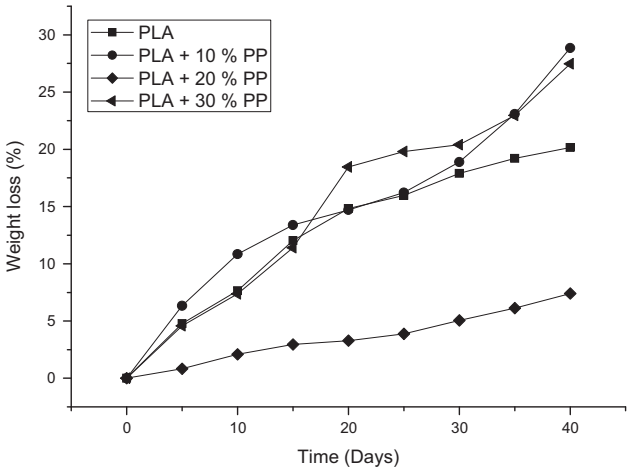

Fig. 7. Weight loss vs. incubation time in PBS for porous *P. purpureum*/PLA scaffolds: (a) PLA_C, (b) PLA/PP_{10}, (c) PLA/PP_{20}, and (d) PLA/PP_{30}.

7.4% of its initial weight. The weight loss trend of the PLA_C, PLA/PP_{10}, and PLA/PP_{30} scaffolds were similar, characterised by a rapid weight loss phase at the initial 15 days, followed by a dramatic weight loss in the remaining weeks. As a result, 20.1%, 28.8%, and 27.4% of the original weights were lost after 40 days of incubation, respectively.

In our study, the weight loss of the PLA_C and PLA/PP_{10} scaffolds increased faster from the early period compared to the PLA/PP_{20} scaffold. Based on FESEM results, we can conclude that the microstructure of the PLA/PP_{10} and PLA_C scaffolds is similar. The larger and wider pore size of the PLA_C and PLA/PP_{10} scaffolds, compared to that of PLA/PP_{20}, might account for the increased weight loss, as the medium could diffuse more easily into the scaffolds. Therefore, we concluded that the PLA_C and PLA/PP_{10} scaffolds displayed a faster degradation than PLA/PP_{20} in accordance with the literature (Niu et al., 2009; You et al., 2005; Mansourizadeh et al., 2014). Wu et al. reported that scaffolds with larger pore sizes tend to degrade more quickly (i.e., are less resistant to hydrolysis) than those with smaller pore sizes. The reason is that they possess thicker pore walls and therefore a smaller surface area to volume ratio, which delay the diffusion of small chains (acidic-by-products), resulting in a stronger acid-catalysed (auto-catalysed) hydrolysis (Wu and Ding, 2004). Additionally, if the adhesion is weak, the PLA/PP_{10} scaffold has poor strength and fatigue properties. In this study, PBS medium was found to diffuse quickly along the interface of the *P. purpureum*/PLA scaffold owing to insufficient adhesion, which disturbs the interface and leads to rapid strength loss of the scaffolds.

Generally, the development of sufficient adhesion between the matrix and reinforcement is still a challenge in composite science. The PLA/PP_{20} scaffold exhibited reduced degradation compared to the PLA_C, PLA/PP_{10}, and PLA/PP_{30} scaffolds. Moreover, the addition of 20 wt% of *P. purpureum* into a PLA composite scaffold increased the water absorption from 175% to 245%, demonstrating the moisture effect of the *P. purpureum* additives. It is well known that fibre-matrix bonding generated on the scaffold surface can act as a load bearer and improve thermal stability (Liao and Cui, 2004). It has been described that the hydrolytic chain cleavage precedes preferentially in the semi-crystalline regions of PLA, and thus leads to an increase in composite crystallinity (Niu et al., 2009). Therefore, the well-dispersed *P. purpureum* particles helped the medium easily enter the inside of the PLA/PP_{20} scaffold from the interface between the *P. purpureum* particles and PLA matrix. Degradation of semi-crystalline regions of the PLA matrix within the PLA/PP_{20} scaffold occurred prior to the crystalline regions. When the polymer chains in semi-crystalline regions are degraded, the number of semi-crystalline regions decreases and the percentage of crystalline to semi-crystalline regions increases. Thus, the increased *P. purpureum* is expected to reduce the degradation of the PLA/PP_{20} scaffold. This might be due to small molecules produced by the first degradation of grafted PLA molecules onto *P. purpureum* particles that played a role of plasticizer and thus improved the toughness of the PLA/PP_{20} scaffold. Small molecules produced by the slower degradation of the PLA/PP_{20} scaffold also played a role of plasticizer and improved the toughness of the PLA/PP_{20} scaffold to some extent.

However, after 40 days of incubation, it was found that overloading *P. purpureum* fillers could increase the degradation of the PLA/PP_{30} scaffold. The weight loss of the PLA/PP_{30} scaffold gradually increased with further addition of *P. purpureum* content due to the tendency of fillers to agglomerate; some of the fillers would not have been fully enclosed within the composite scaffolds and would have protruded from the surface of the scaffolds. With the *in vitro* degradation results, we can conclude that the interface between *P. purpureum* and the PLA matrix in the PLA/PP_{20} scaffold was more susceptible to erosion by the PBS medium. Based on the mechanical, water absorption, weight loss, and FESEM morphology data obtained from our *in vitro* testing, which was performed in a controlled environment using PBS as a medium, we believe that these results are in agreement with the behaviour observed during *in vivo* in cartilage tissue repair. We found in a few studies that the cartilage has a low regenerative capacity; therefore, chondrocytes need to be expanded in culture and seeded onto a scaffold that is able to degrade slowly and resorb as the new tissue structures grow *in vitro* and/or *in vivo* (Hutmacher, 2000). According to the present study, the PLA/PP_{20} scaffold seems to be suitable in the treatment of artificial cartilage where the fixation needs a slow degradation rate and high water absorption.

3.4.3. Morphology of the P. purpureum/PLA scaffolds before and after in vitro degradation

The morphology of the scaffolds was analysed by FESEM, before and after degradation with different *P. purpureum* contents (Fig. 8). The surface of the composite scaffolds were documented before degradation (Fig. 8(a), (c), (e), and (g)). After the immersion of scaffolds in PBS solution, the surface of the scaffolds had fissures as a result of degradation (Fig. 8(b), (d), (f), and (h)) and also a rougher surface. No obvious morphological changes were observed in the PLA_C and PLA/PP_{10} scaffolds for up to 40 days. In contrast, the PLA/PP_{20} and PLA/PP_{30} scaffolds did change at the end of degradation. The microstructure of the degraded PLA/PP_{20} scaffold is shown in Fig. 8(f). When degraded for 40 days, both the size and number of the pores decreased and some fibre-like connections appeared among the pores. The pore morphology on the surface of the PLA/PP_{30} scaffold is shown in Fig. 8(f). At the end of 40 days degradation, most of the pores disappeared and the remaining pores were shrunken with an obvious fibre-like connection present among the pores. The change in morphology of the PLA/PP_{30} scaffold was similar to that of the PLA/PP_{20} scaffold, but the microstructure changes happened earlier in the degradation period as it degraded faster. The results highlight that the microstructure of the PLA/PP_{30} scaffold is rougher as compared with the PLA_C, PLA/PP_{10}, and PLA/PP_{20} scaffolds. This could be attributed to the overloading of *P. purpureum* content in the composite scaffold. The formulation with higher *P. purpureum* content could result in more exposed *P. purpureum* surface, leading to severe weight loss of the scaffold in PBS due to the behaviour of filler that may be protruding from the surface of the scaffold.

4. Conclusion

Biodegradable composites with different content of *P. purpureum* as filler were successfully prepared via the solvent casting and particulate leaching technique and characterised. The scaffolds had a well-interconnected structure and high porosity with pore size varying from 68 to 204 μm. The *P. purpureum* fillers were exposed and dispersed well on the surface of scaffolds according to FESEM images. However, the compression strength and modulus of a *P. purpureum*/PLA scaffold

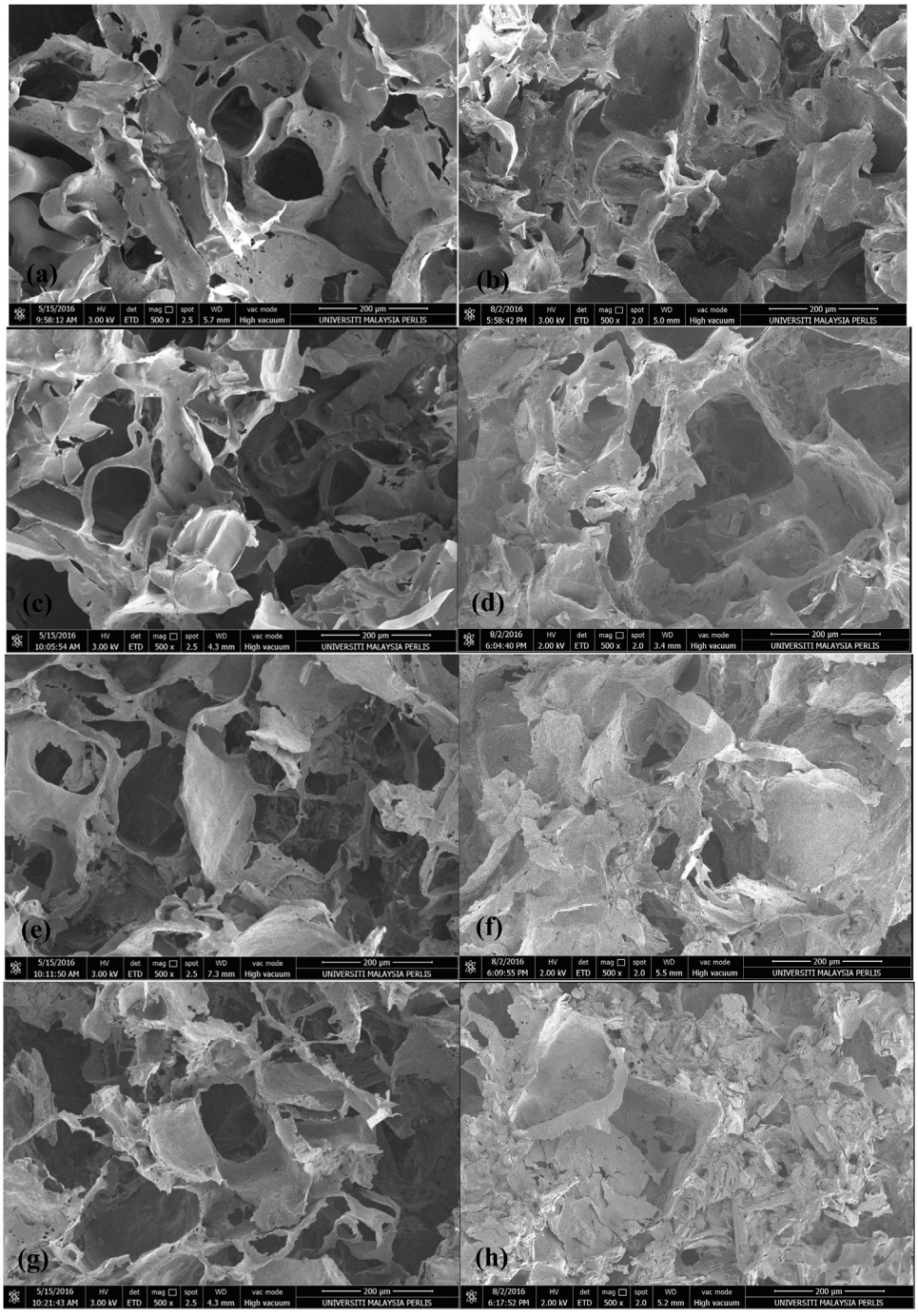

Fig. 8. FESEM micrographs of the morphology of P. purpureum/PLA scaffolds before and after degradation, respectively: (a and b) PLA_C, (c and d) PLA/PP_{10}, (e and f) PLA/PP_{20}, and (g and h) PLA/PP_{30}.

increased with higher fibre loadings through transferring a reinforcement effect within the PLA scaffolds. At the end of 40 days, the pH value of the PLA/PP_{20} and PLA/PP_{30} scaffolds was kept nearly identical at 7.33 and 7.34, respectively. *In vitro* degradation testing revealed that of the three composites and pure PLA scaffold, the PLA/PP_{20} scaffold exhibited the expected bioactivity for cartilage regeneration. Biodegradation results demonstrated that the reinforcement with *P. purpureum* could increase the water absorption of PLA scaffolds and greatly influence the degradation rate of the PLA matrix. According to the described results, the favourable mechanical strength and *in vitro* degradation of the PLA/PP_{20} scaffold has the potential to provide an ideal environment for cell attachment and tissue formation in cartilage tissue engineering applications.

Funding

This work was supported by the Ministry of Education, Malaysia through the Fundamental Research Grant Scheme (FRGS) 2015 (grant number 9003-00566).

Acknowledgement

The authors thank the School of Mechatronic Engineering, Universiti Malaysia Perlis for the use of its facilities.

References

AL-Oqla, F.M., Sapuan, S.M., Anwer, T., Jawaid, M., Hoque, M.E., 2015. Natural fiber reinforced conductive polymer composites as functional materials: a review. Synth.

Met. 206, 42–54. http://dx.doi.org/10.1016/j.synthmet.2015.04.014.
Bogoeva-Gaceva, G., Avella, M., Malinconico, M., Buzarovska, A., Grozdanov, A., Gentile, G., Errico, M.E., 2007. Natural fiber eco-composites. Polym. Compos. 28, 98–107. http://dx.doi.org/10.1002/pc.20270.
Cen, L., Liu, W.E.I., Cui, L.E.I., Zhang, W., Cao, Y., L, R.S.W., People, S., Tong, S.J., 2008. Collagen tissue engineering: development of novel biomaterials. Pediatr. Res. 63, 492–496.
Chandramohan, Marimuthu, 2011. Characterization of natural fibers and their application in bone grafting substitutes. Acta Bioeng. Biomech. 13, 77–84.
Chen, G., Ushida, T., Tateishi, T., 2002. Scaffold design for tissue engineering. Macromol. Biosci. 2, 67–77. http://dx.doi.org/10.1002/1616-5195(20020201)2:2<67::AID-MABI67>3.0.CO;2-F.
Chen, Q., Bruyneel, A., Clarke, K., Carr, C., Czernuszka, J., 2012. Collagen-based scaffolds for potential application of heart valve tissue engineering. J. Tissue Sci. Eng. S11, 1–6. http://dx.doi.org/10.4172/2157-7552.S11-003.
Cheung, H., Ho, M., Cardona, F., 2009. Natural fibre-reinforced composites for bioengineering and environmental engineering applications. Compos. Part B Eng. 40, 655–663. http://dx.doi.org/10.1016/j.compositesb.2009.04.014.
Cordonnier, T., Sohier, J., Rosset, P., Layrolle, P., 2011. Biomimetic materials for bone tissue engineering - State of the art and future trends. Adv. Eng. Mater. 13, B135–B150. http://dx.doi.org/10.1002/adem.201080098.
Fakhrul, T., Islam, M.A., 2013. Degradation behavior of natural fiber reinforced polymer matrix composites. Procedia Eng. 56, 795–800. http://dx.doi.org/10.1016/j.proeng.2013.03.198.
Gentile, P., Chiono, V., Carmagnola, I., Hatton, P.V., 2014. An overview of poly(lactic-co-glycolic) acid (PLGA)-based biomaterials for bone tissue engineering. Int. J. Mol. Sci. 15, 3640–3659. http://dx.doi.org/10.3390/ijms15033640.
Gupta, B., Revagade, N., Hilborn, J., 2007. Poly(lactic acid) fiber: an overview. Prog. Polym. Sci. 32, 1–84. http://dx.doi.org/10.1016/j.progpolymsci.2007.01.005.
Haameem, M., Abdul Majid, M.S., Afendi, M., Marzuki, H.F.A., Hilmi, E.A., Fahmi, I., Gibson, A.G., 2016. Effects of water absorption on Napier grass fibre/polyester composites. Compos. Struct. 144, 138–146. http://dx.doi.org/10.1016/j.compstruct.2016.02.067.
Haameem, M.J.A., Majid, M.S.A., Afendi, M., Marzuki, H.F.A., Fahmi, I., Gibson, A.G., 2016. Mechanical properties of Napier Grass Fibre / Polyester Composites. Compos. Struct. 136, 1–10. http://dx.doi.org/10.1016/j.compstruct.2015.09.051.
Haameem J.A., M., Majid, M.S. Abdul, Afendi, M., Marzuki, H.F.A., Fahmi, I., Gibson, A.G., 2016. Mechanical properties of Napier grass fibre/polyester composites. Compos. Struct. 136, 1–10. http://dx.doi.org/10.1016/j.compstruct.2015.09.051.
Hetal Patel*, G.S.D., 2011. Minal bonde, biodegradable polymer scaffolds for tissue engineering, trends biomater. Artif. Organs. 25, 20–29. 〈http://www.nature.com/nbt/journal/v12/n7/abs/nbt0794-689.html〉.
Hong, Z., Reis, R.L., Mano, J.F., 2008. Preparation and in vitro characterization of scaffolds of poly(l-lactic acid) containing bioactive glass ceramic nanoparticles. Acta Biomater. 4, 1297–1306. http://dx.doi.org/10.1016/j.actbio.2008.03.007.
Hoveizi, E., Nabiuni, M., Parivar, K., Rajabi-Zeleti, S., Tavakol, S., 2014. Functionalisation and surface modification of electrospun polylactic acid scaffold for tissue engineering. Cell Biol. Int. 38, 41–49. http://dx.doi.org/10.1002/cbin.10178.
Huang, W., Shi, X., Ren, L., Du, C., Wang, Y., 2010. PHBV microspheres - PLGA matrix composite scaffold for bone tissue engineering. Biomaterials. 31, 4278–4285. http://dx.doi.org/10.1016/j.biomaterials.2010.01.059.
Hutmacher, D.W., 2000. Scaffolds in tissue engineering bone and cartilage. Biomaterials. 21, 2529–2543. http://dx.doi.org/10.1016/S0142-9612(00)00121-6.
Izadifar, Z., Chen, X., Kulyk, W., 2012. Strategic design and fabrication of engineered scaffolds for articular cartilage repair. J. Funct. Biomater. 3, 799–838. http://dx.doi.org/10.3390/jfb3040799.
Jeong, S.I., Krebs, M.D., Bonino, C.A., Khan, S.A., Alsberg, E., 2010. Electrospun alginate nanofibers with controlled cell adhesion for tissue engineering. Macromol. Biosci. 10, 934–943. http://dx.doi.org/10.1002/mabi.201000046.
Komistek, R.D., Kane, T.R., Mahfouz, M., Ochoa, J.A., Dennis, D.A., 2005. Knee mechanics: a review of past and present techniques to determine in vivo loads. J. Biomech. 38, 215–228. http://dx.doi.org/10.1016/j.jbiomech.2004.02.041.
Liao, S.S., Cui, F.Z., 2004. In Vitro and in Vivo Degradation of Mineralized Collagen-Based Composite Scaffold: Nanohydroxyapatite/Collagen/Poly(L-lactide). Tissue Eng. 10, 73–80. http://dx.doi.org/10.1089/107632704322791718.
Lopes, M.S., Jardini, A.L., Filho, R.M., 2012. Poly (lactic acid) production for tissue engineering applications. Procedia Eng. 42, 1402–1413. http://dx.doi.org/10.1016/j.proeng.2012.07.534.
Mansourizadeh, F., Mirir, V., Shahabi, F., Mansourizadeh, F., Pasban, E., Asadi, A., 2014. In vitro degradation of electrospinning PLLA/HA nanofiber scaffolds compared with pure PLLA. Int. J. Plant, Anim. Environ. Sci. 4, 330–334.
Naseri, N., Lenart, G., Kristiina, O., 2016. 3-Dimensional porous nanocomposite scaffolds based on cellulose nanofibers for cartilage tissue engineering: tailoring of porosity and mechanical performance. R. Soc. Chem. 6, 5999–6007. http://dx.doi.org/10.1039/C5RA27246G.
Neppalli, R., Causin, V., Marigo, A., Meincken, M., Hartmann, P., Van Reenen, A.J., 2013. Effect of electrospun ethylene vinyl alcohol copolymer (EVOH) fibres on the structure, morphology, and properties of poly(lactic acid) (PLA). Polym. (United Kingdom). 54, 5909–5919. http://dx.doi.org/10.1016/j.polymer.2013.08.046.
Niu, X., Feng, Q., Wang, M., Guo, X., Zheng, Q., 2009. In vitro degradation and release behavior of porous poly(lactic acid) scaffolds containing chitosan microspheres as a carrier for BMP-2-derived synthetic peptide. Polym. Degrad. Stab. 94, 176–182. http://dx.doi.org/10.1016/j.polymdegradstab.2008.11.008.
Oh, S.E.H., Kang, S.G.O.N., Lee, J.I.N.H.O., 2006. Degradation behavior of hydrophilized PLGA scaffolds prepared by melt-molding particulate-leaching method: comparison with control hydrophobic one. J. Mater. Sci. Mater. Med. 17, 131–137.
Olivas-armendariz, I., Santos-Rodríguez, E., Alvarado-Gutiérrez, L.E., Meléndez-Molina, M.L., Márquez-Chávez, Z.A., Valencia-Gómez, L.A., Vargas-Requena, C.L., Martel-Estrada, S.A., 2015. 1In, Biocomposites scaffolds for bone tissue engineering. Int. J. Compos. Mater. 5, 167–176. http://dx.doi.org/10.5923/j.cmaterials.20150506.05.
Razak, S.I.A., Sharif, N.F.A., Rahman, W.A.A., 2012. Biodegradable polymers and their bone applications: a review. Int. J. Basic Appl. Sci. 12, 31–49 http://www.ijens.org/IJBAS Vol 12 Issue 01.html.
Revati, R., Majid, M.S.A., Ridzuan, M.J.M., Normahira, M., Nasir, N.F.M., Rahman, M.N.Y., Gibson, A.G., 2017. Mechanical, thermal and morphological characterisation of 3D porous Pennisetum purpureum / PLA biocomposites scaffold. Mater. Sci. Eng. C. 75, 752–759. http://dx.doi.org/10.1016/j.msec. 2017.02.127.
Ridzuan, M.J.M., Majid, M.S.A., Afendi, M., Kanafiah, S.N.A., Zahri, J.M., Gibson, A.G., 2016. Characterisation of natural cellulosic fibre from Pennisetum purpureum stem as potential reinforcement of polymer. JMADE. 89, 839–847. http://dx.doi.org/10.1016/j.matdes.2015.10.052.
Ridzuan, M.J.M., Abdul Majid, M.S., Afendi, M., Azduwin, K., Amin, N.A.M., Zahri, J.M., Gibson, A.G., 2016. Moisture absorption and mechanical degradation of hybrid Pennisetum purpureum/glass-epoxy composites. Compos. Struct. 141, 110–116. http://dx.doi.org/10.1016/j.compstruct.2016.01.030.
Ridzuan, M.J.M., Abdul Majid, M.S., Afendi, M., Aqmariah Kanafiah, S.N., Zahri, J.M., Gibson, A.G., 2016. Characterisation of natural cellulosic fibre from Pennisetum purpureum stem as potential reinforcement of polymer composites. Mater. Des. 89, 839–847. http://dx.doi.org/10.1016/j.matdes.2015.10.052.
Ridzuan, M.J.M., Abdul Majid, M.S., Afendi, M., Aqmariah Kanafiah, S.N., Zahri, J.M., Gibson, A.G., 2016. Characterisation of natural cellulosic fibre from Pennisetum purpureum stem as potential reinforcement of polymer composites. Mater. Des. 89, 839–847. http://dx.doi.org/10.1016/j.matdes.2015.10.052.
Ridzuan, M.J.M., Majid, M.S.A., Afendi, M., Mazlee, M.N., Gibson, A.G., 2016. Thermal behaviour and dynamic mechanical analysis of Pennisetum purpureum/glass-reinforced epoxy hybrid composites. Compos. Struct. 152, 850–859. http://dx.doi.org/10.1016/j.compstruct.2016.06.026.
Shah, A.R., Shah, S.R., Oh, S., Ong, J.L., Wenke, J.C., Agrawal, C.M., 2011. Migration of co-cultured endothelial cells and osteoblasts in composite hydroxyapatite/polylactic acid scaffolds. Ann. Biomed. Eng. 39, 2501–2509. http://dx.doi.org/10.1007/s10439-011-0344-z.
Tian, H., Tang, Z., Zhuang, X., Chen, X., Jing, X., 2012. Biodegradable synthetic polymers: preparation, functionalization and biomedical application. Prog. Polym. Sci. 37, 237–280. http://dx.doi.org/10.1016/j.progpolymsci.2011.06.004.
Tu, C., Cai, Q., Yang, J., Wan, Y., Bei, J., Wang, S., 2003. The fabrication and characterization of poly(lactic acid) scaffolds for tissue engineering by improved solid-liquid phase separation. Polym. Adv. Technol. 14, 565–573. http://dx.doi.org/10.1002/pat.370.
Vogt, S., Larcher, Y., Beer, B., Wilke, I., Schnabelrauch, M., 2002. Fabrication of highly porous scaffold materials based on functionalized oligolactides and preliminary results on their use in bone tissue engineering. Eur. Cells Mater. 4, 30–38.
Wu, L., Ding, J., 2004. In vitro degradation of three-dimensional porous poly(D,L-lactide-co-glycolide) scaffolds for tissue engineering. Biomaterials. 25, 5821–5830. http://dx.doi.org/10.1002/jbm.a.30487.
You, Y., Min, B.-M., Lee, S.J., Lee, T.S., Park, W.H., 2005. In vitro degradation behavior of electrospun polyglycolide, polylactide, and poly(lactide-co-glycolide). J. Appl. Polym. Sci. 95, 193–200. http://dx.doi.org/10.1002/app.21116.
Zhang, L., Hu, J., Athanasiou, K.A., 2009. The role of tissue engineering in articular cartilage repair and regeneration. Crit. Rev. Biomed. Eng. 37, 1–57. http://dx.doi.org/10.1016/j.pestbp.2011.02.012.Investigations.
Zhang, Z., Cui, H., 2012. Biodegradability and biocompatibility study of poly(chitosan-g-lactic acid) scaffolds. Molecules. 17, 3243–3258. http://dx.doi.org/10.3390/molecules17033243.
Zhu, N., Cooper, D., Chen, X.-B., Niu, C.H., 2013. A study on the in vitro degradation of poly(l-lactide)/chitosan microspheres scaffolds. Front. Mater. Sci. 7, 76–82. http://dx.doi.org/10.1007/s11706-013-0188-6.